J Mater Sci (2010) 45:3344–3349
DOI 10.1007/s10853-010-4355-1

On the free volume kinetics during isochronal structural relaxation of Pd-based metallic glass: effect of temperature and deformation

K. Hajlaoui · M. A. Yousfi · Z. Tourki · G. Vaughan · A. R. Yavari

Received: 11 November 2009 / Accepted: 25 February 2010 / Published online: 12 March 2010
© Springer Science+Business Media, LLC 2010

Abstract Free volume changes of amorphous $Pd_{42.5}Cu_{30}Ni_{7.5}P_{20}$ due to structural relaxation under isochronal heat treatments have been quantified using in situ synchrotron X-ray diffraction measurements. The analysis of the first diffraction peak position during the annealing process has allowed us to follow the free volume change during relaxation. The data obtained were successfully fitted to relaxation equations based on free volume model (FVM) and the drawn conclusion is that the FVM remain a useful tool for describing the relaxation phenomena in metallic glasses well below glass transition. The effect of deformation and temperature on kinetics of structural relaxation of the amorphous structure has been quantitatively investigated.

K. Hajlaoui (✉) · A. R. Yavari
SIMaP-LTPCM, Institut National Polytechnique de Grenoble, 38402 Saint Martin d'Heres, France
e-mail: khalil.hajlaoui@eniso.rnu.tn; k.hajlaoui@yahoo.fr

K. Hajlaoui
LGM-MA05, ENIM, Av. Ibn El Jazzar, 5019 Monastir, Tunisia

K. Hajlaoui
Ecole Nationale d'Ingénieurs de Sousse, Avenue 18 janvier, 4000 BabJdid, Tunisia

M. A. Yousfi · Z. Tourki
LMMP LAB-STI03, Université de Tunis, ESSTT, 1008 Tunis, Tunsia

G. Vaughan
European Synchrotron Radiation Facilities (ESRF), 38402 Grenoble, France

Introduction

As metallic glasses (MGs) are produced by very rapid quenching from the liquid state, the as-quenched glass will contain a large amount of free volume and metallic glass is very far from equilibrium. Upon heating at sufficiently high temperatures where some atomic mobility is possible, the glass tends to lower its free energy and relaxes towards the metastable equilibrium state along a path which is dependent on its thermal history. This process is generally called structural relaxation and manifested by changes in all physical properties [1]. These changes can be understood in view of the reduction of free volume that occurs during a pre-annealing treatment [2]. The reduction of the amount of free volume causes a lower defect concentration, giving rise to a higher viscosity [3, 4], a higher density [5], a higher tensile strength and causes severe embrittlement [6–8]; some hypoeutectic glassy alloys exhibit a high resistance against the embrittlement caused by structural relaxation [9, 10]. Therefore, striking a balance between the metallic bond nature and free volume is a suitable approach to enhance the toughness and ductility of glassy alloys.

The processes of annihilation of free volume during structural relaxation can experimentally be determined directly by measuring density, length (volume) and average positron lifetime changes [11] of amorphous alloys under isothermal and non-isothermal conditions. Density measurements of bulk amorphous alloys were presented by Inoue [12] and Nagel et al. [13]. The volume expansion of the amorphous $Pd_{40}Cu_{30}Ni_{10}P_{20}$ alloy was measured by Lu et al. [14] using the sessile drop method with an advanced high resolution image analysis. The results of these papers show that the density changes of the amorphous alloy due to structural relaxation are directly connected with changes

in the free volume. Unfortunately, no attempt has been made to discuss this interdependence quantitatively and only limited research has been conducted to quantify the structural relaxation that occurs in these alloys during thermal ageing. The limited investigations into the structural relaxation of MGs result from their poor thermal stability in the undercooled liquid region. Due to this poor stability, the glasses would rapidly crystallise upon annealing above the glass transition temperature T_g. However, the discovery of new composition of MGs that possess a high resistance to crystallization in the undercooled liquid region has led to increased studies of the behaviour of MGs in the glass transition region. In addition, it is generally known that the change in the amorphous structure is very small during relaxation, especially at lower temperature. Therefore, careful experiments and techniques are necessary to realise such a specific study and special emphasis must be made to improve the precision of the measurements.

The aim of this study is to measure directly the free volume of amorphous samples of $Pd_{42.5}Cu_{30}Ni_{7.5}P_{20}$ under isochronal heating (linear heating) and to demonstrate that the experimental results can be described quantitatively using the FVM model. We present in situ synchrotron X-ray diffraction measurements that allow us to study the free volume change during annealing of MGs. The effect of temperature and high strain deformation on kinetics of structural relaxation of the amorphous structure will be quantitatively investigated.

Experimental details

The $Pd_{60}Ni_{40}$ alloy was first prepared by sintering 99.99% Pd and 99.9995% P in an evacuated quartz tube. Then, the master alloy of the composition of $Pd_{42.5}Cu_{30}Ni_{7.5}P_{20}$ was produced by arc melting a mixture of the $Pd_{60}Ni_{40}$ alloy and the elements Pd, Ni (99.993%) and Cu (99.99%). Fully glassy rods of composition of $Pd_{42.5}Cu_{30}Ni_{7.5}P_{20}$ (at.%), 10 mm in diameter, were obtained from the Institute for Materials Research, Tohoku University, Japan [15]. ribbon samples with 40μm thickness and 2 mm width were prepared from a part of the crushed bulk glass by an ordinary melt-spinning apparatus. Ribbon-like samples of the same alloy were produced at SIMaP-Grenoble, France. A detailed description of the equipment and the procedure used is given in Ref. [16]. The amorphous nature of the samples was carefully checked by X-ray diffraction measurements, employing a diffractometer operating with Cu K_α radiation.

For this work, glassy $Pd_{42.5}Cu_{30}Ni_{7.5}P_{20}$ is chosen because of its excellent glass-forming ability and high thermal stability against crystallization [15, 17], providing a suitable way to study and understand the nature of structural relaxation. Segments of the ribbons of about 10 mm in length were heated from room temperature to 593 K (above T_g) at a rate of 40 K/min, then cooled at the same rate down to around 373 K and heated up again until crystallization. The temperature was measured and controlled by the thermocouple of a commercial Linkam hot stage. To consider the effect of deformation on structural relaxation, like-foil packs were obtained by low amplitude milling of the melt-spun ribbons in a vibratory mill with a single 6 cm diameter ball under argon gas and obtained foils was used for the same heat treatment cycle.

Now, to follow in real time the structure evolution of MGs, synchrotron radiation X-ray diffraction in transmission was carried out during in situ heating–cooling–heating cycle. We used a high energy monochromatic beam on the ID11 beam line of the European Synchrotron Radiation Facility (ESRF) [18] equipped with a nitrogen-cooled double-silicon monochromator. The photon energy was 90 keV corresponding to an X-ray wave length of about 0.0137 nm. The total intensity elastically scattered by the samples I(Q) (Q scattering vector) was obtained subtracting background and applying absorption, multiple scattering, and inelastic Compton scattering corrections using the values provided by Cromer and Mann [19] and the so-called Breit recoil factor. The generalised Krogh–Moe–Norman method [20] with the atomic scattering factors tabulated in [21] and including the anomalous dispersion corrections [22] were used to normalise the intensity data. Further technical details on experimental set-up were given in previous publications [23–27].

Experimental results and discussion

Primary results consist of a succession of XRD patterns of $Pd_{42.5}Cu_{30}Ni_{7.5}P_{20}$ glassy ribbon subjected to various temperatures during continuous heating as shown in Fig. 1. The position of the first maximum of diffraction intensity (Q_{max}) is noted to slightly shift to a higher wave-vector (Q) with decreasing temperature as a result of thermal expansion.

To analyse the observed feature and as it is known in the case of crystalline material, the scattering vector Q equals to $2\pi/d_{hkl}$ for interplanar distances d_{hkl}. By analogy ΔQ on heating is related to $2\pi/\Delta d$, where d is the mean interatomic distance for the glassy material. According to Yavari and coworkers [23–27] the change in the position of the centre of mass of the first diffraction maximum Q_{max} in Q corresponds to the change of the mean interatomic distance in the first coordination shell provided that all of the interactions are elastic. As the glassy phase is isotropic the variation in $Q_{max}(T^0)/Q_{max}(T)$ ($Q_{max}(T^0)$ being the first diffraction maximum value at room temperature) was

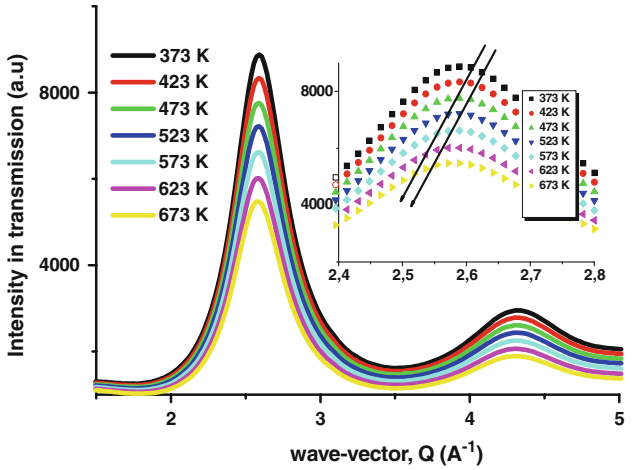

Fig. 1 Representative synchrotron radiation XRD patterns of the glassy $Pd_{42.5}Cu_{30}Ni_{7.5}P_{20}$ alloy at different temperatures. The *inset* shows close-ups of the top of the first diffraction maximum of the glass

found to scale with the change in the reduced average interatomic distance d_T/d_T^0 and thus, with the linear size changes L_T/L_T^0. The change in the reduced average volume per atom V_T/V_T^0 scales with the variation in $(Q_{max}(T^0)/Q_{max}(T))^3$:

$$V(T)/V(T^0) = \left(Q_{max}(T^0)/Q_{max}(T)\right)^3 \quad (1)$$

Hence, precise measurements of the Q_{max} changes allow direct measurement of the reduced average volume per atom evolution in the samples.

Now, to obtain Q_{max} values, the upper half of the first broad diffraction peak was cut from the data and fitted with a peak-type function, for example, Lorentzian or Voigt function. In Fig. 2a the selected Q-region that was used for fitting is noted by the vertical and horizontal dashed lines and Fig. 2b show the best fit with a Lorentz function of the first diffuse scattering peak. The resulting centre of mass data for the diffraction peaks collected for each temperature during heating–cooling cycle $Q_{(T)}$ were then normalised to $Q_{max}(T^0)/Q_{max}(T)$ ($Q_{max}(T^0)$ equal to 2.59334 ± 0.00044 A^{-1}).

Based on the above peak determination method one can indicate that the precision of the specific volume per atom value measured by the shift of the diffraction maximum with temperature depend upon the precision with which the centre of mass of the first diffraction maximum has been found by Lorentzian fitting. Furthermore, the good fitting quality of the broad diffraction peak as shown in Fig. 2b (coefficient of determination equal to 0.9985) gives the Q-value at the centroid of the fitted peak from diffraction patterns with a relative error around 0.015%. The error in finding the centre of mass is connected with a slightly nonsymmetrical shape of the main maximum peak.

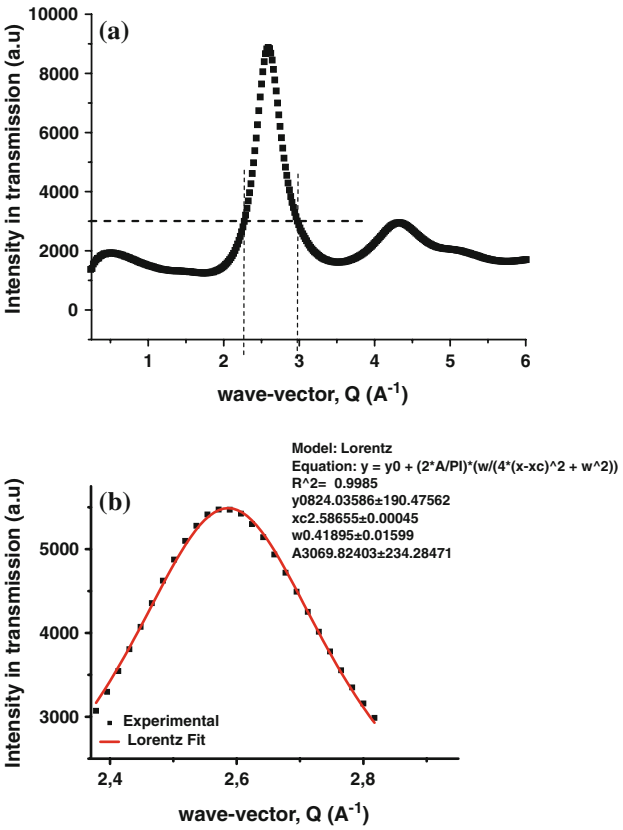

Fig. 2 **a** Diffraction pattern of the sample at a given temperature during heating–cooling cycle. The region of the pattern that was fit with a Lorentz peak is denoted by the *dashed lines*. **b** Lorentz fit of first scattering maxima

Figure 3a shows the reduced volume change computed using Eq. 1. As shown in this figure, an initial linear thermal dilatation zone is followed by structural relaxation. More quantitative analyses dealing with the volume coefficients of thermal expansion α_{th} and glass transition temperature T_g were well developed in our previous papers [23, 24].

This work focuses mainly on analysing the quantitative measurement of annealing-out free volume (or excess free volume $\Delta V_f(T)$) during structural relaxation which can be obtained by the difference, taken for each temperature, between the as-quenched and the annealed ribbon (see arrows in Fig. 3a). Figure 3b presents the calculated excess free volume changes during isochronal structural relaxation in $Pd_{42.5}Cu_{30}Ni_{7.5}P_{20}$ metallic glass. As shown in Fig. 3b, the initial value of excess free volume $\Delta V_{f,0}$ obtained for $Pd_{42.5}Cu_{30}Ni_{7.5}P_{20}$ glassy ribbon is around 0.2% which shows a good agreement with the results of melt-spun MGs measured by dilatometry [28] and creep measurements [29]. Compared to as-quenched ribbon, the excess free volume trapped into the deformed foils sample is higher (more than 0.3%), which is in agreement with the well-known deformation-induced free volume established in a number of works [30–32].

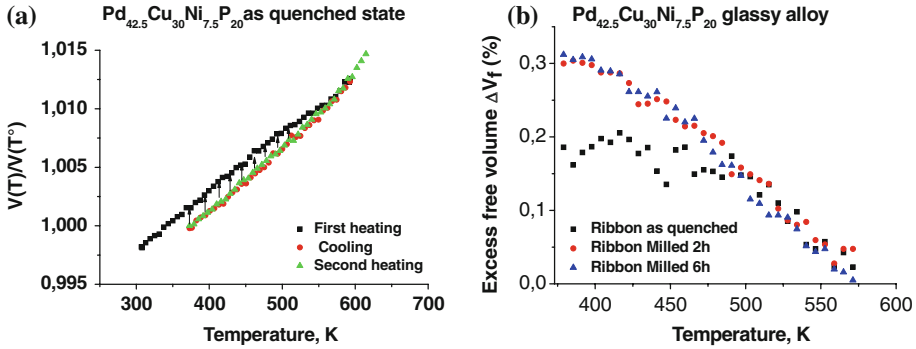

Fig. 3 **a** Mean atomic volume change of amorphous metallic ribbons during a heating–cooling-heating cycle at 40 K/min. **b** The excess free volume change occurred during structural relaxation of as-quenched ribbon and heavily deformed foils of the $Pd_{42.5}Cu_{30}Ni_{7.5}P_{20}$

When the sample is heated at a constant heating rate, the structure relaxes towards equilibrium and free volume gradually decreases (Fig. 3b) according to the kinetic which appears dependent on the temperature and the deformation. It seems that the structural relaxation of deformed specimen began at a lower temperature than the as-cast ribbon glass. This is yet consistent with an increase in free volume due to plastic deformation, which pushes the system further out of equilibrium and provides a larger driving force for relaxation. Theoretical calculations of free volume evolution during isochronal annealing conducted by Van Den Beukel and Radellaar [33] give almost the same set of curve as in Fig. 3b. In addition, the free volume reduction measured by our X-ray method is well correlated with enthalpy change according to the scheme proposed by Van Den Beukel and Sietsma [34]. Heating of the material during the DSC experiment leads to an increase of the atomic mobility and the decrease of the free volume ΔV_f is accompanied by a decrease of the enthalpy of the material. As a result, a low-temperature exothermic effect should appear in the temperature range of about 425–575 K and 400–575 K for as-quenched ribbon and foils, respectively. Relaxed free volume in the sample can in principal be restored by continuing heating above T_g [34] leading to an increase of the enthalpy of the sample, and an endothermic peak appears in the DSC trace which is identified as the glass transition. However, we have not seen such behaviour because in our constant heating rate experiment the kinetics of free volume production seems to be too sluggish to keep up with the constantly increasing temperature, and hence ΔV_f undershoots the equilibrium behaviour.

Constitutive equations and parametric identification of structural relaxation

The free volume model (FVM) was commonly used to explain the structural relaxation. Based on FMV, the free volume annihilation during annealing can be well established by the second-order kinetics [35, 36]:

$$(dC_f/dt) = -k\,C_f^2; \quad C_f(t=0) = C_{f,0} \tag{2}$$

where $C_f = \exp(-\gamma\, v^*/v_f)$ is the concentration of the flow defects, it relates to the so-called reduced free volume $v_f/\gamma v^*$ according to Ref. [37] and where γv^* is approximated to 0.5 Ω [34] (Ω is the atomic volume) and v_f is the mean free volume per atom.

The concentration of the flow defect can be related to measured ΔV_f according to $C_f = \exp(-\gamma\, v^*/v_f) \approx \exp(-\gamma/\Delta V_f)$, where ΔV_f have nearly the same significance as v_f/v^*. $k(T) = C_0 \exp(-Q_r/RT)$, Q_r is the activation energy and C_0 is the atomic jump frequency. Equation 2 only accounts for the annihilation of 'defects'. However, close to equilibrium, the production part can not longer be omitted and several possibilities to adapt Eq. 2 have been considered [38]. To prevail one of these equations for the description of free volume changes requires a precise measurement of free volume above T_g which is still experimentally difficult. While the choice of consistent equation is still the matter of debate and under consideration, it has been shown [38] that the most suitable differential equation describing the change of C_f with time is given by:

$$(dC_f/dt) = -k\,C_f\left(C_f - C_{f,eq}\right) \tag{3}$$

where $C_{f,eq}$ is the equilibrium defect concentration given by a Fulcher–Vogel type equation $C_{f,eq} = \exp(-B/(T - T_0))$, where B and T_0 are two model parameters.

We shall use the above equation to explain the structural relaxation data obtained by X-ray diffraction measurements.

Under isochronal structural relaxation conditions at a constant heating rate $q = dT/dt$ the reduced free volume $X = v_f/v^* \approx \Delta V_f$ can be described by:

$$\frac{dX}{dT} = -\frac{C_0}{q\cdot\gamma}\cdot\exp\left(-\frac{Q_r}{R;T}\right)\cdot X^2\cdot\left[\exp\left(-\frac{\gamma}{X}\right) - \exp\left(-\frac{B}{T-T_0}\right)\right] \tag{4}$$

Equation 4 includes several physical parameters, namely Q_r, C_0, B and T_0 which can be obtained by fitting this equation to our X-ray relaxation measurements of Fig. 3b. This equation is then fitted to free volume change

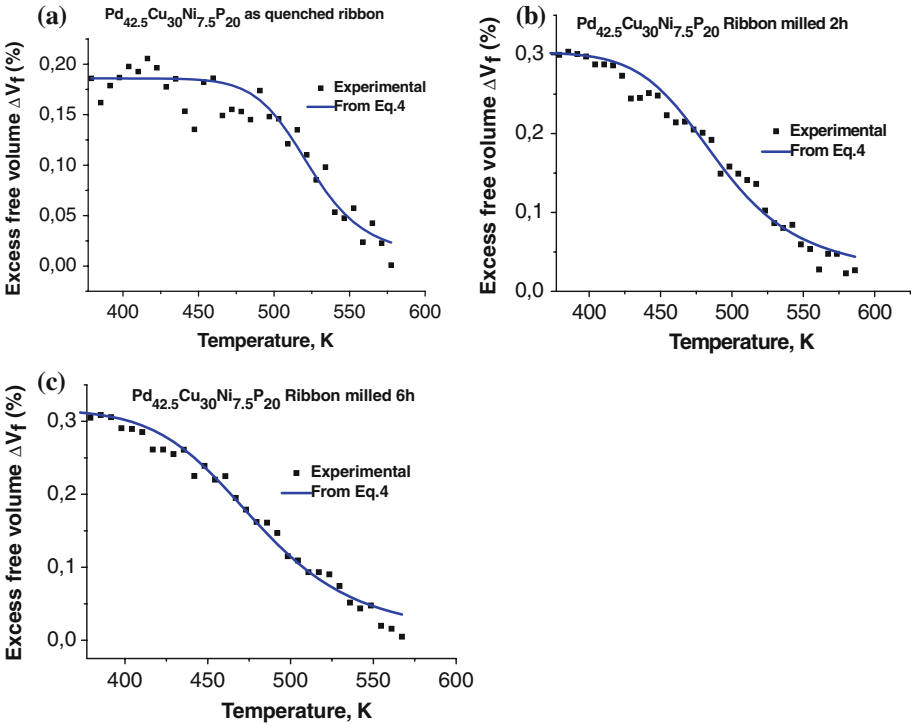

Fig. 4 Decrease of free volume during isochronal annealing of $Pd_{42.5}Cu_{30}Ni_{7.5}P_{20}$ glassy ribbon together with the best fit curve obtained on the basis of Eq. 4 at a heating rate of 40 K/min: **a** for as-cast ribbon; **b**, **c** for deformed ribbon

during annealing. Figure 4a–c shows the experimentally obtained temperature dependence of free volume of the studied glassy alloy (for strained and unstrained ribbon) together with the best fit curve obtained on the basis of Eq. 4 at a heating rate of 40 K/min. The values of the fitting parameters are given in Table 1.

As it is seen in Fig. 4, Eq. 4 is qualified to describe the relaxation experimental data when interpreting the results on the basis of FVM. Almost of adjustable model parameters obtained in this study are physically meaningful and comparable with those found by other authors using other measurement methods as viscosity, length and density changes [5]. Activation energy for relaxation is seen to be decreasing for deformed ribbon and this feature is due to the existence of favoured atomic 'hole' (induced by high deformation) making more easily the multi-atomic cooperative rearrangements caused by thermal effect. The activation energy for atomic motion is therefore decreased due to the large driving force for relaxation. Work to identify the significance of obtained model parameters is ongoing.

To summarise, the basic features of structural relaxation behaviours in MGs can be attributed to different origins: kinetics of free volume relaxation [this work], compositional/topological short-range ordering [39, 40], some peculiarities of the activation energy spectra [41, 42] and change of the structural factor [43, 44]. In a separate work, a wide range of relaxation data obtained by diffraction methods will be used to study the mentioned origins of structural relaxation in various compositions of MGs.

Table 1 Parameters as obtained by fitting the X-ray experimental data according to Eq. 4 at a heating rate of 40 K/min for strained and unstrained state of $Pd_{42.5}Cu_{30}Ni_{7.5}P_{20}$ ribbon. Results from literature were also presented for comparison

	As-quenched ribbon	Ribbon milled 2 h	Ribbon milled 6 h	From literature Ref. [5]
C_0 (s^{-1})	4×10^{11}	10^7	10^5	3.12×10^{19}
Q_r (kJ/mol)	121.19	66.84	54.4	130.45
T_0 (K)	379	331	349	307
B (K)	6148	8485	8879	6324
γ	0.039	0.107	0.029	0.8

Conclusion

1 Free volume changes of the amorphous $Pd_{42.5}Cu_{30}Ni_{7.5}P_{20}$ alloy have been measured directly during isochronal heating conditions using precise in situ synchrotron X-ray diffraction measurements.
2 The FVM provides a simple description for structural relaxation phenomena below and close to the glass transition temperature T_g.
3 The deformed Pd-based glass has exhibited structural relaxation at a lower temperature, indicative of a higher initial free volume produced by plastic deformation or by rapid cooling from liquid state. Kinetics of structural relaxation is governed by the temperature and the amount of free volume content.

Acknowledgement K.H. gladly acknowledges a European Marie Curie Ph.D. fellowship in the frame-work of the RTN Network "Ductile BMG Composites" coordinated by ARY.

References

1. Khonik VA, Kosilov AT, Mikhailov VA, Sviridov VV (1998) Acta Mater 46:3399
2. Spaepen F (1981) In: Poirier JJ, Kleman M (eds) Physics of defects, Les Houches Lectures XXXV. North Holland, Amsterdam, p 135
3. Waniuk TA, Busch R, Masuhr A, Johnson WL (1998) Acta Mater 46:5229–5236
4. Yokoyama Y, Ishikawa T, Okada JT, Watanabe Y, Nanao S, Inoue A (2009) J Non-Cryst Solids 355:317
5. Russew K, Sommer F (2003) J Non-Cryst Solids 319:289
6. Yokoyama Y, Yamasaki T, Liaw PK, Inoue A (2008) Acta Mater 56:6097
7. Greer AL (1984) J Non-Cryst Solids 61–62:737
8. Yokoyama Y, Akeno Y, Yamasaki T, Liaw PK, Buchanan RA, Inoue A (2005) Mater Trans 46:2755
9. Yoshida N, Fujita K, Yokoyama Y, Kimura H, Inoue A (2007) J Jpn Inst Met 71:730
10. Yokoyama Y, Yamasaki T, Nishijima N, Inoue A (2007) Mater Trans 48:1276
11. Ishii A, Hori F, Iwase A, Fukumoto Y et al (2008) Mater Trans JIM 49:1975
12. Inoue A (1998) Materials science foundation 4. TransTech, Switzerland
13. Nagel C, Ratzke K, Schmidtke E, Wolff J, Geyer U, Faupel F (2000) Phys Rev B 57:10225
14. Lu IR, Gorler GP, Fecht HJ, Willnecker R (2000) J Non-Cryst Solids 274:294
15. Inoue A, Nishiyama N, Matsuda T (19961) Mater Trans JIM 37:181
16. Uriarte JL (2004) Les Verres Metalliques Massif. PhD Thesis, Institut National Polytechnique de Grenoble
17. Li N, Liu L, Zhang M (2009) J Mater Sci 44:3072. doi: 10.1007/s10853-009-3407-x
18. ESRF Beamline ID11, www.esrf.fr
19. Cromer DT, Mann JB (1967) J Chem Phys 47:1892
20. Waseda Y (1980) The structure of non-crystalline materials. McGraw-Hill Inc., New York
21. Ibers JA, Hamilton WC (eds) (1974) International tables for X-ray crystallography, vol IV. Birmingham, Kynoch Press (present distributor Kluwer Academic Publishers, Dordrecht), p 148
22. Cromer DT, Liberman DL (1970) J Chem Phys 53:1891
23. Hajlaoui K, Benameur T, Vaughan G, Yavari AR (2004) Scripta Mater 51:843
24. Yavari AR, Le Moulec A, Inoue A, Nishiyama N et al (2005) Acta Mater 53:1611
25. Yavari AR, Inoue A, Botta WJ, Kvick A (2001) Scripta Mater 44:1239
26. Yavari AR, LeMoulec A, Inoue A, Botta WJ, Vaughan G, Kvick A (2001) Mater Sci Eng A 34:304
27. Louzguine DV, Yavari AR, Ota K, Vaughan G, Inoue A (2005) J Non-Cryst Solids 351:1639
28. Chen HS (1978) J Appl Phys 49:3289
29. Taub AI, Spaepen F (1980) Acta Mater 28:1781
30. Li Jing, Spaepen F, Hufnagel TC (2002) Philos Mag A 82:2623
31. Li Jing, Wang ZL, Hufnagel TC (2002) Phys Rev B 65:144201
32. Wright WJ, Hufnagel TC, Nix WD (2003) J Appl Phys 93:3
33. Van Den Beukel A, Radelaar S (1983) Acta Mater 31:419
34. van den Beukel A, Sietsma J (1990) Acta Metall Mater 38:383
35. Tsao SS, Spapen F (1985) Acta Mater 33:881
36. Volkert CA, Spaepen F (1989) Acta Mater 37:1355
37. Turnbull D, Cohen MH (1961) J Chem Phys 34:120
38. Duine PA, Sietsma J, Van Den Beukel A (1992) Acta Mater 40:743
39. Haruyama O, Tando M, Kimura HM, Nishiyama N, Inoue A (2002) J Non-Cryst Solids 603:312
40. Kokmeijer E, Huizer E, Thijsse BJ, Van den Beukel A (1988) Phys Status Solidi A 105:235
41. Fritsh G, Shulte A, Wohlfart J, Schuster J, Lüscher E (1988) J Less-Common Metals 145:339
42. Sietsma J, Baricco M (1991) Mater Sci Eng A 133:518
43. Kelton KF, Spaepen F (1984) Phys Rev B 30:5516
44. Mattern N, Sakowski J, Kühn U, Vinzelberg H, Eckert J (2004) J Non-Cryst Solids 345–346:758